Old Dominion University

ODU Digital Commons

2023

Levels of Autotrophy and Heterotrophy in Mesophotic Corals Near the End Photic Zone

Amy Carmignani

Veronica Z. Radice
Old Dominion University, vradice@odu.edu

Kathryn M. McMahon

Alex I. Holman

Karen Miller

See next page for additional authors

Follow this and additional works at: https://digitalcommons.odu.edu/biology_fac_pubs

Part of the Climate Commons, Marine Biology Commons, and the Terrestrial and Aquatic Ecology Commons

Original Publication Citation

Authors

Amy Carmignani, Veronica Z. Radice, Kathryn M. McMahon, Alex I. Holman, Karen Miller, Kliti Grice, and Zoe Richards

Check for updates

Levels of autotrophy and heterotrophy in mesophotic corals near the end photic zone

Amy Carmignani[1*†], Veronica Z. Radice[2], Kathryn M. McMahon[3], Alex I. Holman[4], Karen Miller[5], Kliti Grice[4] and Zoe Richards[1,6]

[1]Coral Conservation and Research Group, Trace and Environmental DNA Laboratory, School of Molecular and Life Sciences, Curtin University, Bentley, WA, Australia, [2]Department of Biological Sciences, Old Dominion University, Norfolk, VA, United States, [3]Centre for Marine Ecosystems Research, School of Science, Edith Cowan University, Joondalup, WA, Australia, [4]Western Australian Organic and Isotope Geochemistry Centre, The Institute for Geoscience Research, School of Earth and Planetary Sciences, Curtin University, Perth, WA, Australia, [5]Australian Institute of Marine Science, Crawley, WA, Australia, [6]Collections and Research, Western Australian Museum, Welshpool, WA, Australia

Mesophotic corals live at ~30-150 m depth and can sustain metabolic processes under light-limited conditions by enhancing autotrophy through specialized photoadaptations or increasing heterotrophic nutrient acquisition. These acclimatory processes are often species-specific, however mesophotic ecosystems are largely unexplored and acclimation limits for most species are unknown. This study examined mesophotic coral ecosystems using a remotely operated vehicle (Ashmore Reef, Western Australia at $40-75m$ depth) to investigate the trophic ecology of five species of scleractinian coral (from genera *Leptoseris*, *Pachyseris*, and *Craterastrea*) using stable isotope analyses ($\delta^{13}C$ and $\delta^{15}N$) of host and symbiont tissues and protein concentration. Trophic strategies were analyzed between species and between overall corals sampled above and below the end-photic point, where light is only 1% of surface irradiance. Results showed species-specific differences in resource use. *Leptoseris hawaiiensis*, *L. scabra*, and *P. speciosa* had similar $\Delta^{13}C$ values ($\delta^{13}C$ host - $\delta^{13}C$ symbiont) approaching zero (< 0.5 ‰) which indicated greater dependence on symbiont autotrophy. In contrast, *Leptoseris glabra* and *Craterastrea levis* had higher $\Delta^{13}C$ values (1.4 to 3.5 ‰) which indicated a greater reliance on external carbon sources. The latter two species also demonstrated tight nitrogen recycling within the holobiont, exhibiting low $\Delta^{15}N$ values (host $\delta^{15}N$ - symbiont $\delta^{15}N$ =< 0.5 ‰), compared to more autotrophic species ($\Delta^{15}N$ = >1.2 ‰). Some species demonstrated the ability to maintain metabolic processes despite substantially reduced light availability (0.5 − 2% of surface irradiance). This research challenges our knowledge of acclimation limits for many scleractinian corals and contributes novel information for Ashmore Reef, the Western Australia region and mesophotic ecosystems in general, and critically examines common methods used to interpret trophic ecology with bulk stable isotopes $\delta^{13}C$ and $\delta^{15}N$.

1 Introduction

Mesophotic coral reef ecosystems (MCEs) harbor scleractinian corals between ~30 to 150 m depth where light availability is reduced compared to shallow water. Many scleractinian corals rely on photoautotrophic nutrient input via symbiotic intracellular algae (Symbiodiniaceae) to meet metabolic demands in oligotrophic waters (Baker, 2003; Muller-Parker et al., 2015). Thus, light availability is the primary factor driving vertical coral ecology (Mass et al., 2010; Kahng et al., 2019; Tamir et al., 2019) and biodiversity changes over depth (López-Londoño et al., 2022). As corals are mixotrophic they can also acquire organic nutrients through heterotrophy by the active or passive capture of plankton or particulate organic matter (Lewis and Price, 1975; Sebens et al., 1996). Some coral species are depth-generalists, surviving from shallow water down to upper mesophotic depths (to ~60 m). In contrast, depth-specialist corals typically inhabit low-light, mesophotic environments (below ~60 m) (Bongaerts et al., 2015; Lesser et al., 2019) and have been recorded at 172 m depth (*Leptoseris hawaiiensis*, French Polynesia) (Rouzé et al., 2021). Increasing heterotrophic nutrient acquisition can compensate for potential photosynthetic deficiencies under low light availability (*e.g.*, turbid waters, seasonal environmental changes, and depth) (Anthony andFabricius, 2000; Ferrier-Pagès et al., 2011; Kahng et al., 2019), provisioning longer-term energy reserves (Seemann et al., 2012; Tremblay et al., 2015) compared to rapidly metabolised photosynthates (Tremblay et al., 2015). However, the understanding of metabolic trade-offs at depth remains unclear and investigations into the trophic plasticity and photoadaptations of mesophotic Scleractinia under various environmental conditions are still in their infancy.

Interest in MCEs has accelerated over the last decade (reviewed in Turner et al., 2017) due to technical advances (*e.g.*, remotely operated vehicles (ROVs), autonomous underwater vehicles (AUVs) and imaging technology) (Muir et al., 2015; Armstrong et al., 2019; Pinheiro et al., 2019) and interest in the Deep Reef Refuge Hypothesis (DRRH), which suggests MCEs may function as short-term ecological refuges, long term refugia or deep areas of resilience for threatened corals (Glynn, 1996; Riegl and Piller, 2003; Bongaerts and Smith, 2019). Despite this, mesophotic corals remain poorly studied when compared to shallow reefs (< 30 m) (Kahng et al., 2014; Turner et al., 2017; Eyal et al., 2021), and available literature is geographically biased towards the northern hemisphere regions (*i.e.*, Atlantic, Red Sea, and Caribbean) (Turner et al., 2017; Muir and Pichon, 2019). Little is known about mesophotic ecosystems in the Indo-Pacific and northwest Australian regions, despite hosting some of the world's most extensive reef systems with the highest coral species richness globally (Laverick et al., 2018; Muir and Pichon, 2019). Furthermore, physiological studies predominantly use common species from shallower waters such as *Stylophora pistillata* (Reynaud et al., 2002; Alamaru et al., 2009; Einbinder et al., 2009; Houlbrèque and Ferrier-Pagès, 2009; Mass et al., 2010) and *Montastraea cavernosa* (Vize, 2006; Lesser et al., 2007; Lesser et al., 2010; Serrano et al., 2014), hence there is a dearth of literature for the majority of mesophotic scleractinian corals (Loya et al., 2019). Understanding how mesophotic corals can

survive in only a fraction of shallow reef irradiance (Englebert et al., 2017; Hoeksema et al., 2017) is an essential part of understanding their ecophysiology and limitations (Loya et al., 2016). Symbiodiniaceae can translocate up to 95% of their photosynthates to coral hosts (Sutton and Hoegh-Guldberg, 1990), yet corals can also increase heterotrophic reliance to supplement for metabolic deficits (Muscatine et al., 1989; Lesser et al., 2010; Sturaro et al., 2021) as photosynthate production slows over depth (Mass et al., 2010; Kahng et al., 2019).

Whole tissue (bulk) stable isotope analysis (SIA) of carbon (δ^{13}C) and nitrogen (δ^{15}N) provides information about the trophic ecology and dietary contributions of corals (Muscatine et al., 1989; Reynaud et al., 2002; Lesser et al., 2010; Tremblay et al., 2015). The δ^{13}C values of coral host tissues typically reflect those of key nutrient sources, such as photosynthates from symbionts or external carbon sources obtained heterotrophically from the water column (*i.e.*, plankton and particulate organic matter) (Peterson and Fry, 1987; Muscatine et al., 1989; Kahng et al., 2019). Therefore, larger deviations in δ^{13}C between the coral host and symbionts indicate the incorporation of external nutrients. The process of photosynthesis preferentially fixes lighter carbon isotopes (^{12}C) (Muscatine et al., 1989), thus symbionts with higher photosynthetic rates have higher δ^{13}C values (*i.e.*, in shallow waters) (Muscatine et al., 1989; Reynaud et al., 2002; Lesser et al., 2010). Subsequently, δ^{13}C values of symbionts (and the overall holobiont) typically decrease gradually with increasing depth in response to light reductions that lower photosynthetic fractionation (Heikoop et al., 1998; Lesser et al., 2010). Low host δ^{13}C values can also result from heterotrophic feeding and may reflect the δ^{13}C values of particulate resources such as phytoplankton and zooplankton (-17 ‰ to -21 ‰) (Land et al., 1975; Fontugne and Claude Duplessy, 1978; Rodrigues and Grottoli, 2006).

In typical food webs, an estimated average δ^{15}N enrichment of approximately +2 to 3.4 ‰ occurs in consumers with each trophic level (Minagawa and Wada, 1984; Lesser et al., 2010) and has previously been used to assess levels of heterotrophy in corals. This enrichment estimation, however, incorporates averages from various taxa and environments (including terrestrial and freshwater) (Minagawa and Wada, 1984; Zanden and Rasmussen, 2001). In addition to this, there are no overall trends between δ^{15}N and heterotrophy in mesophotic corals (Lesser et al., 2022), likely due to multiple nitrogen inputs (Mullin et al., 1984) and nitrogen recycling (Reynaud et al., 2009; Tremblay et al., 2015; Rangel et al., 2019), however this relationship has been largely unstudied. Complementary physiological/metabolic measurements (*e.g.*, dietary biomarkers, protein analysis, photosynthetic proxies) can strengthen the interpretation of SIA and trophic strategies (Houlbrèque et al., 2003; Ferrier-Pagès et al., 2011; Crandall et al., 2016; Radice et al., 2019a), yet species-specific physiological adaptations and metabolic trade-offs at depth should also be considered (Houlbrèque and Ferrier-Pagès, 2009; Cooper et al., 2011a; Cooper et al., 2011b; Seemann, 2013; Brunner, 2015).

Western Australia includes a vast marine realm spanning over 30 degrees of latitude where important coral biodiversity hotspots have been identified in shallow waters (< 30 m) of the north-west

region (*e.g.*, Scott Reef, Ashmore Reef) (Richards et al., 2014). To date, few studies have analyzed mesophotic coral physiology in the extended Western Australian region (Cooper et al., 2011a; Cooper et al., 2011b) and, to our knowledge, the physiology of mesophotic corals at Ashmore Reef has never been examined. This study aimed to determine the levels of autotrophy and heterotrophy in mesophotic coral species using SIA of carbon (δ^{13}C) and nitrogen (δ^{15}N) and protein analyses. As the sampling range extends into the lower mesophotic depths, it is hypothesized that in general, coral species will require the input of external nutrient sources to sustain their metabolic budget at depth necessitated by low light levels. It is also hypothesized that *P. speciosa*, a known obligate autotroph (Veron, 2000), will differ to the depth-specialist species of the genera *Leptoseris* and *Craterastrea*. Here, we provide a first assessment of *in-situ* trophic ecology in depth-specialists *Craterastrea levis*, *Leptoseris glabra*, *Leptoseris hawaiiensis*, *Leptoseris scabra* and depth-generalist *Pachyseris speciosa* for Western Australia. This research also provides valuable information on the limits of acclimation of Indo-Pacific mesophotic corals and the trophic capabilities of zooxanthellate corals at depth.

2 Materials and methods

2.1 Sample collection

Ashmore Reef is an exposed, oceanic reef situated in the Timor Sea along Australia's north-west shelf, 460 km north of the Dampier Peninsula on Australia's mainland (Supplementary Figure 1A). Sample collections were conducted at Ashmore Reef, Western Australia (12°13'45"S 123°02'15"E) on the R/V *FALKOR* between 12 and 24 April 2021, as part of the Mesophotic Coral Examination hosted by Schmidt Ocean Institute in collaboration with the Australian Institute of Marine Science, University of Western Australia, Western Australian Museum and Curtin University. Coral sampling was conducted at six sites around the reef between 41 – 75 m (Supplementary Figure 1B) (Permit Number AU-COM2021-508). Sites were chosen to encompass habitats around as much of the reef as possible to align with shallow reef monitoring sites (Gilmour et al., 2019), however the most eastern side of the reef was not accessible for sampling due to strong currents. *Leptoseris* spp. and *Pachyseris* sp. were target taxa based on their known presence at mesophotic depths in NW Australia (Cooper et al., 2011a; Cooper et al., 2011b; Turner et al., 2018; Heyward and Radford, 2019; Muir and Pichon, 2019). April marks the beginning of the dry season, and conditions during all sampling days were calm with no cloud cover.

Coral fragments (~5 cm length) were sampled using the Remotely Operated Vehicle (ROV) *SUBASTIAN* and stored in solid quivers, in seawater from the collection site (*i.e.*, same water temperature), for the duration of the dive (~1.5 - 7 hours), where no light reached the samples. Few samples were alternatively stored in transparent boxes on the ROV. Subsequently, all samples were immediately transferred to the lab and only samples stored in quivers (where there was no light interaction) were measured for

dark-adapted quantum yield (Fv/Fm). Fragments for SIA and protein analysis were subsampled and rinsed with filtered seawater (FSW) (0.45 μm Millipore filters through an EZ-STREAM® vacuum pump) to remove any extraneous particles or debris and frozen at -80°C.

The species were identified based on skeletal morphology as *Leptoseris hawaiiensis*, *Leptoseris glabra*, *Leptoseris scabra*, *Craterastrea levis* and *Pachyseris speciosa*. All sample information (*e.g.*, species, depth, site) is detailed in Supplementary Tables 1, 5.

2.2 Environmental variables

CTD casts (Biospherical Quantum Sensor, LI-COR) recorded downwelling profiles of solar irradiance (photosynthetically active radiation (PAR) μmol m^{-2} s^{-1}) (McCree, 1981), temperature (°C) (ITS-90), and chlorophyll-*a* (mg^{-1} m^{-3}) (WET Labs ECO-AFL/FL). An overall mean PAR by depth was calculated from midday (11:30am - 12:30pm) from two CTD casts (sites 2W and 3NW) and when solar irradiance was highest (Mass et al., 2010; Kirk, 2011; Tamir et al., 2019). This informed mean mid-photic and end-photic points that occur at 10% and 1% of surface PAR, respectively (Lesser et al., 2010; Kirk, 2011). To further describe the light environment at Ashmore Reef, a mean vertical diffuse attenuation coefficient of downwelling light (PAR$_{Kd}$) was calculated according to Lambert-Beer law ($I_z = I_0 e^{Kdz}$) defined by Kirk (2011). PAR$_{Kd}$ is primarily influenced by solar incidence (Brakel, 1979; Lesser et al., 2019), scattering, and absorption of light in the water column (Kirk, 2011; Muir and Pichon, 2019). Due to logistical issues and challenging current conditions, not all environmental variables were obtained from each site (Supplementary Table 2). It is acknowledged that temporal differences in cast times could influence readings.

2.3 Taxonomic identifications

Skeletal vouchers were taxonomically examined to identify species based on the accepted names in the World Register of Marine Species (https://www.marinespecies.org - 12.08.2021). Identifications were made after viewing macro and microstructural features and with reference to the following literature (Dinesen, 1980; Veron, 2000; Benzoni et al., 2012; Arrigoni et al., 2019). Whole skeletal images were taken with a Cannon EOS80D DSLR Camera, and macro images with a Leticia LAS X camera. Scanning electron microscopy (SEM) was undertaken on select specimens using the Vega3 Tescan Variable Pressure microscope (HV: 20kV, BI 10.00) in the John de Laeter Centre at Curtin University, Western Australia.

2.4 Ecophysiology

2.4.1 Photo-physiology

Dark-adapted quantum yield of photosystem II (Fv/Fm) of each colony was measured to determine coral health at the time of

sampling. This was carried out using a Dive Pulse-Amplitude-Modulated (PAM) Fluorometer (Diving-PAM, Walz Gmbh, Germany) with the saturation pulse method (Genty et al., 1989; Schreiber, 2004) within 45 minutes after reaching the surface. Corals were only taken out of the quivers briefly (~30 seconds) to perform PAM measurements under a low artificial light (~1 – 2 μmol photons m^{-1} s^{-1}). Average values were taken from three measurements of the outer, central, and inner sections of each colony (>20 mm apart) to capture intracolonial variation in chlorophyll distribution (Ralph et al., 2005). The fiberoptic cable was held directly onto the coral coenosarc (the most planar surface) as a standardization of optical distance (0 mm), in order to minimize potential variation in fluorescence (Ralph et al., 2005).

2.4.2 Stable isotope analysis (SIA)

The methodology used for SIA was an adaptation of Einbinder et al. (2009) and Reynaud et al. (2002). Samples were thawed from -80°C and holobiont material comprising the animal host tissue (host) and algal symbionts (symbiont) was removed by gently airbrushing (OZITO 3 L 105 W airbrush) with a reservoir of 10 - 15 mL FSW (0.45 μm) at a maximum of 4 psi. The holobiont slurry was initially centrifuged (Heraeus Multifuge X1R Centrifuge, Thermo Scientific) at 4°C at 3000 g for 5 minutes to separate the host tissue from the symbiont pellet. Mucousy samples that did not separate on initial centrifugation were homogenized using a handheld tissue homogenizer (D-9, MICCRA) for 30 - 60 seconds on 11,000 rpm and centrifuged again at 3000 g for 5 minutes (Sturaro et al., 2019). The host supernatant was centrifuged again (3 times) at 4°C at 3000 g for 5 minutes and purity was checked under a compound microscope. The symbiont pellet was resuspended in 2 mL of FSW and centrifuged again at 3000 g for 5 minutes. The supernatant was discarded, and this process was repeated 2 - 3 times before checking for purity.

The symbiont components were acidified with 1 N HCl to remove any residual carbonates (e.g., skeletal fragments). The acid was added dropwise with a pipette until bubbling ceased (Sturaro et al., 2019). Acidified samples were sonicated for 10 minutes before being repeatedly washed with FSW and centrifuged at 3000 g for 5 minutes until supernatant pH = 7 (neutral). Any white top layer that may comprise host lipids and excess liquid was removed with a pipette. Samples were freeze-dried (Alpha 1-2 LD plus Freeze-Dryer, Martin Christ) for >24 hours.

Triplicates of the dried host and symbiont material (~0.2 mg for symbiont and ~0.2 - 0.6 mg for host tissue) were encapsulated in tin cups (3.5 × 5 mm, Eurovector) and combusted to CO_2 and N_2 in an Elemental Analyzer (Flash 2000 HT, Thermo Scientific) coupled to an Isotope Ratio Mass Spectrometer (DELTA V Advantage Mass Spectrometer, Thermo Scientific) via a ConFlow IV to measure stable isotope ratios of carbon ($^{13}C/^{12}C$) and nitrogen ($^{15}N/^{14}N$) as $\delta^{13}C$ and $\delta^{15}N$ in per mil (Western Australian Organic & Isotope Geochemistry Centre labs, Curtin University, Australia) for host (n = 30) and symbiont (n = 30) samples. The instrument was calibrated by running triplicate blanks and duplicates of certified reference materials USGS40 (L-glutamic acid), USGS41 (L-glutamic acid) (Qi et al., 2003), and IAEA-600 (caffeine) (Coplen et al., 2006),

before and after each full sample batch. Instrumental analytical precision for carbon and nitrogen was 0.1 ± 0.08 ‰ and 0.1 ± 0.09 ‰, respectively. SIA values for individual samples were averaged from triplicates and conventionally expressed as delta (δ) values in parts per mil (‰) as deviations relative to the Vienna Peedee Belemnite Limestone Standard (V-PDB) for C and atmospheric nitrogen gas (N_2) for N (Peterson and Fry, 1987; Coplen, 2011; Ben-David and Flaherty, 2012).

$$\delta \ (‰) = \left(\left(\frac{sample^{ratio}}{standard^{ratio}} \right) - 1 \ \times 1000 \right)$$

2.4.3 Host protein concentrations

Aliquots for protein analysis were obtained from final host supernatant samples by pipetting 0.5 mL of host tissue into a 20 mL glass vial, diluted with 2 μL of FSW and stored at -20°C prior to analysis. The absorbance of samples was measured in triplicate by adding 2 μL of tissue to a Nanodrop 1000 Spectrophotometer (software V3.8) to obtain average absorbances at λ 235 nm and 280 nm (setting: ProteinA280; sample type: universal mg/mL). The instrument was repeatedly calibrated to $Milli\text{-}Q^{®}$ water and FSW was used as a control for the possible presence of proteins in the dilutant. Calculations to determine concentrations followed those by (Whitaker and Granum, 1980) to account for interference of other nucleic and amino acids.

$$\frac{\lambda\, 280nm - \lambda\, 235nm}{2.51}$$

Data were normalized to the surface area of the coral airbrushed. Surface area measurements were taken using the foil method as in (Marsh, 1970). Four 100 cm^2 (10 cm x 10 cm) squares of foil were cut and measured to obtain a mean weight for 100 cm^2, then the area for 1 cm^2 calculated. Final protein concentration (mg/mL) per cm^2 of skeletal surface area was calculated as:

$$\frac{protein\ concentration\ (mg\ mL^{-1}) \times airbrushed\ volume\ (mL)}{Surface\ area\ (cm^2)}$$

The foil method has come under critique for overestimating the surface area of branching and rounded morphologies due to significant foil overlapping (Hoegh-Guldberg, 1988; Veal et al., 2010), yet all corals in this study exhibited flat, simple morphologies which avoided overlapping.

2.5 Statistical analysis

All analyses were conducted in R (v1.4.1717). Data were inspected visually to check normality and homogeneity using histogram charts and sample quantile plots (RStudio Team, 2020). Linear Mixed Effects (LME) models ('nlme') were used to test for effects of species, species and tissue type, or depth and species with site included as a random effect.

Sampling was not fully replicated across species and depths due to the opportunistic sampling method, challenges with environmental conditions and patchy habitat distribution in

Ashmore's mesophotic reef. Subsequently, analyses were performed for overall means for either species or irradiance level. Corals were separated into two irradiance levels: above 1% of surface irradiance (above 1% SI), which included corals from 45 – 54 m depths (n = 11), and below 1% of surface irradiance (below 1% SI), which included corals from 55 – 75 m depths (n = 19). These groups represent corals living above and below the mean end-photic point, which occurs when light levels reach just 1% of surface irradiance.

One outlier was removed from the analysis of protein (*L. hawaiiensis* < 55 m depth). The difference in stable isotopes between individual paired host and symbiont samples ($\Delta^{13}C$ and $\Delta^{15}N$) were also tested (*e.g.*, host $\delta^{13}C$ – symbiont $\delta^{13}C$). Significance levels were based on $\alpha = 0.05$. *Post-hoc* Tukey pairwise tests were analyzed for significant results ('emmeans'). Means are ± 1 Standard Deviation. Pearson's correlation tests were used to test relationships between depth vs. symbiont $\delta^{13}C$, symbiont $\delta^{15}N$ and protein. Ellipse plots of isotopic niches ($\delta^{13}C$ vs. $\delta^{15}N$) were plotted based on a 40% confidence interval representing the maximum likelihood standard ellipse area (Jackson et al., 2011). All raw data are contained in Supplementary Table 5.

3 Results

3.1 Environmental characterization

Solar irradiance (PAR) followed an exponential decline over depth. Mean surface PAR was 2245 μmol m^{-2} s^{-1} (at 1 m) with an average diffuse attenuation coefficient of PAR$_{Kd}$ = 0.069 m^{-1}. Mean mid- (10%) and end-photic (1%) points were realized at 27 m and 54 m, respectively (Supplementary Figure 2). This represents the optical properties of water at Ashmore Reef at time of sampling. Mean sea surface temperature was 29.51 ± 0.12°C (± SE) and gradually decreased over depth by 1.69 ± 0.17°C to 80 m depth (Supplementary Figure 2). This indicated relatively consistent temperatures across the sampled depth range (41 – 75 m). Chlorophyll-*a* fluorescence readings for chlorophyll-a density in the water column represented quantities of phytoplankton across depth. These quantities were highest at mesophotic depths, with all sites exhibiting low phytoplankton concentrations at the surface (< 1 mg m^{-3}) until 25 – 35 m or deeper before peaking at depths approximate to the upper mesophotic zone (30 – 68 m).

3.2 Photo-physiology (dark-adapted quantum yield)

Dark-adapted quantum yields (Fv/Fm) across species ranged from 0.69 - 0.71, which indicated that corals were in healthy condition at the time of sampling (Ralph et al., 2015, *e.g.*, Padilla-Gamiño et al., 2019; Bhagooli et al., 2021). There were species differences detected in Fv/Fm among species ($F_{1,23} = 5.69$, p = 0.002). Pairwise Tukey *post-hoc* test showed *Leptoseris hawaiiensis* (0.71 ± 0.01) had significantly higher Fv/Fm than *P. speciosa* (0.67 ±

0.03) ($t_{19} = 3.411$, p = 0.022) and *L. glabra* (0.67 ± 0.01) ($t_{19} = -3.589$ p = 0.015), yet overall mean values in corals remained constant between depths above and below 1% SI ($F_{1,23} = 0.610$ p = 0.444).

3.3 Coral stable carbon isotope ($\delta^{13}C$) analysis

The coral host and symbiont fractions were analyzed for $\delta^{13}C$ (‰). Mean coral host $\delta^{13}C$ trends showed higher values in *L. glabra* (-19.1 ± 1.5 ‰) and *C. levis* (-19.5 ± 0.7 ‰) compared to *L. hawaiiensis* (-21.3 ± 1.4 ‰), *L. scabra* (-20.1 ± 2.0 ‰), and *P. speciosa* (-20.2 ± 1.2 ‰) (Table 1; Figure 1A), yet these differences were not significant ($F_{4,22} = 2.394$, p = 0.081) (Supplementary Table 4). In contrast, symbiont $\delta^{13}C$ values were lowest in *L. glabra* (-22.6 ± 0.8 ‰) and *C. levis* (-21.0 ± 1.4 ‰) and highest in *L. scabra* (-20.6 ± 1.5 ‰) and *P. speciosa* (-20.7 ± 0.7 ‰) (Table 1; Figure 1B). Linear mixed effects models indicated a significant effect of species ($F_{4,22} = 3.565$, p = 0.022), with Tukey pairwise tests revealing significantly lower symbiont $\delta^{13}C$ in *L. glabra* (-22.6 ± 0.8 ‰) compared to both *L. hawaiiensis* (-20.9 ± 0.7 ‰) ($t_{22} = -3.502$, p= 0.015) and *P. speciosa* (-20.7 ± 0.7 ‰) ($t_{22} = -3.535$, p = 0.014) (Supplementary Table 4).

Differences in host $\delta^{13}C$ were not detected between depths above and below 1% SI ($F_{1,25} = 0.013$, p = 0.909), however overall symbiont $\delta^{13}C$ had a significant relationship with depth and became more negative as depth increased and light availability diminished (correlation= -0.545, $t_{28} = -3.435$, p = 0.002) (Figure 2). Accordingly, corals from depths above 1% SI (-20.3 ± 0.8 ‰) had significantly higher symbiont $\delta^{13}C$ values than corals below 1% SI (-21.4 ± 1.0 ‰) ($F_{1,25} = 7.277$, p = 0.012).

Linear mixed effects models used to test for differences between coral host vs. symbiont $\delta^{13}C$ among species found no significant effect of species ($F_{4,47} = 1.286$, p = 0.289), however there was a significant effect of host *vs.* symbiont tissues ($F_{1,47} = 6.417$, p = 0.015) and an interaction between species and tissue type ($F_{4,47} = 4.401$, p = 0.004) (Supplementary Table 4). Tukey *post-hoc* tests showed that *L. glabra* had higher host $\delta^{13}C$ values (-19.1 ± 1.5 ‰) compared to its symbionts (-22.6 ± 0.8 ‰) ($t_{47} = 4.363$, p = 0.003) (Figure 1A).

The $\Delta^{13}C$ value is the pairwise difference between individual coral host and symbiont $\delta^{13}C$ values and was also tested for differences among species and between irradiance levels. *Leptoseris glabra* (3.5 ± 1.7 ‰) and *C. levis* (1.4 ± 1.0 ‰) had relatively higher $\Delta^{13}C$ compared to all other species (*L. hawaiiensis*, *P. speciosa* and *L. scabra*) that had $\Delta^{13}C$ values below 0.5 ‰. (Table 1; Figure 3A). Linear mixed effects models revealed an effect of species ($F_{4,21} = 4.086$, p = 0.013), with significant differences between in *L. glabra* ($\Delta^{13}C = 3.5 ± 1.7$ ‰) and *L. hawaiiensis* (-0.4 ± 1.7 ‰) ($t_{21} = 3.928$, p = 0.006) (Supplementary Table 4). Mean coral $\Delta^{13}C$ was also analyzed between irradiance levels, with corals above 1% SI exhibiting extremely low mean $\Delta^{13}C$ values (0.1 ± 1.6 ‰), compared to corals below 1% (1.1 ± 2.2 ‰), yet there was a lot of variation within the data and differences between these irradiance levels were not significant ($F_{1,21} = 2.328$, p = 0.142).

TABLE 1 Overall means of stable isotope variables (Host $\delta^{13}C$ and $\delta^{15}N$, Symbiont $\delta^{13}C$ and $\delta^{15}N$, host-symbiont $\delta^{13}C$ ($\Delta^{13}C$), and host-symbiont $\delta^{15}N$ ($\Delta^{15}N$) and protein concentrations in mesophotic corals collected in April 2021 from Ashmore Reef, Western Australia, across species and irradiance levels (over 1% surface irradiance (SI) and under 1% SI).

Species	n	Host $\delta^{13}C$ (‰)	Host $\delta^{15}N$ (‰)	Symbiont $\delta^{13}C$ (‰)	Symbiont $\delta^{15}N$ (‰)	$\Delta^{13}C$ (‰)	$\Delta^{15}N$ (‰)	Protein (mg mL^{-1} cm^{-2})
Craterastrea levis	4	-19.5 ± 0.7	5.4 ± 0.5	-21.0 ± 1.4	5.0 ± 0.6	1.4 ± 1.0	0.5 ± 0.4	1.90 ± 0.47
Leptoseris glabra	4	-19.1 ± 1.5	5.3 ± 0.6	-22.6 ± 0.8	5.0 ± 0.8	3.5 ± 1.7	0.3 ± 1.1	1.49 ± 0.23
Leptoseris hawaiiensis	9	-21.3 ± 1.4	5.8 ± 1.4	-20.9 ± 0.7	3.6 ± 1.3	-0.4 ± 1.7	2.3 ± 1.2	1.50 ± 0.71
Leptoseris scabra	3	-20.1 ± 2.0	6.3 ± 0.7	-20.6 ± 1.5	4.2 ± 0.4	0.5 ± 2.9	2.1 ± 0.6	2.26 ± 0.30
Pachyseris speciosa	10	-20.2 ± 1.2	5.7 ± 1.1	-20.7 ± 0.7	4.4 ± 0.5	0.4 ± 1.5	1.2 ± 1.0	0.97 ± 0.55
Irradiance Level	n	Host $\delta^{13}C$ (‰)	Host $\delta^{15}N$ (‰)	Symbiont $\delta^{13}C$ (‰)	Symbiont $\delta^{15}N$ (‰)	$\Delta^{13}C$ (‰)	$\Delta^{15}N$ (‰)	Protein (mg mL^{-1} cm^{-2})
above 1% SI	11	-20.2 ± 1.1	6.0 ± 1.2	-20.3 ± 0.8	4.5 ± 0.4	0.1 ± 1.6	1.5 ± 1.1	1.65 ± 0.73
below 1% SI	19	-20.3 ± 1.6	5.5 ± 0.9	21.4 ± 1.0	4.2 ± 1.1	1.1 ± 2.2	1.5 ± 1.2	1.34 ± 0.62

Mean values are ± 1 Standard Deviation.

3.4 Coral stable nitrogen isotope ($\delta^{15}N$) analysis

Mean coral host $\delta^{15}N$ values of corals ranged from 5.3 ± 0.6 ‰ (*L. glabra*) to 6.3 ± 0.7 ‰ (*L. scabra*) (Table 1), yet no significant differences occurred among species ($F_{4,22}$ = 0.347, p = 0.844) (Table 1; Figure 1B; Supplementary Table 4). Conversely, there was a significant effect of species on symbiont $\delta^{15}N$ ($F_{4,22}$ = 3.476, p = 0.024). *Craterastrea levis* and *L. glabra* shared the lowest mean symbiont $\delta^{15}N$ (5.0 ± 0.6 ‰ and 5.0 ± 0.8 ‰, respectively) while *L. hawaiiensis* had the highest (3.6 ± 1.3 ‰), however differences were only significant between *L. hawaiiensis* and *L. glabra* (t_{22} = 3.216, p = 0.029) (Figure 1B; Table 1; Supplementary Table 4). Irradiance level did not affect host $\delta^{15}N$ ($F_{1,25}$ = 1.166, p = 0.290) or symbiont
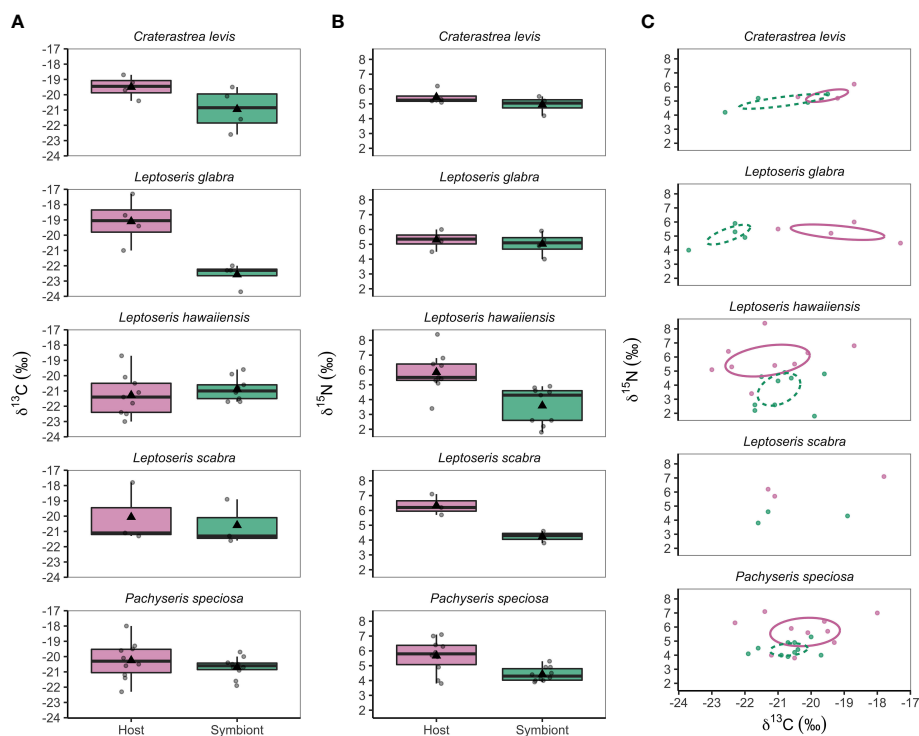
FIGURE 1
(A) Mesophotic coral host (pink) and symbiont (green) $\delta^{13}C$ values, (B) $\delta^{15}N$ values, and (C) isotopic niches of hosts (pink solid line) and symbionts (green dashed line) from five coral species collected between 44 m and 75 m depth from Ashmore Reef, Western Australia. Dots in (C) represent individual data points and ellipses are based on a 40% confidence interval that represent the maximum likelihood standard ellipse area. The sample size of *Leptoseris scabra* (n = 3) was insufficient to calculate an ellipse, however trends in its isotopic niche can be observed.

FIGURE 2
Trends over depth of Symbiont δ^{13}C (44 m to 75 m) recorded in mesophotic coral species in April at Ashmore Reef, Western Australia.

FIGURE 3
(A) Differences between paired δ^{13}C values from individual coral hosts and symbionts (Δ^{13}C) and (B) paired δ^{15}N values from individual coral hosts and symbionts (Δ^{15}N) in five mesophotic coral species (44 m to 75 m depth) from Ashmore Reef, Western Australia.

δ^{15}N ($F_{1,25} = 0.959$, p = 0.337). (Table 1; Figure 1B; Supplementary Table 4). In contrast to symbiont δ^{13}C data, no significant trends were found between symbiont δ^{15}N and depth (correlation = -0.137, t_{28} = -0.734, p = 0.469).

Linear mixed effects models were used to test for differences in δ^{15}N between coral hosts and symbionts among species. Results showed no significant effect of species ($F_{4,47} = 1.024$, p = 0.405), however there was a significant effect of tissue type ($F_{1,47} = 34.803$, p<0.001). Tukey *post-hoc* tests showed that *L. hawaiiensis* host had significantly higher host δ^{15}N (5.8 ± 1.4 ‰) compared to its

symbionts (3.6 ± 1.3 ‰) ($t_{47} = 5.181$, p<0.001) (Table 1; Figures 1B, C; Supplementary Table 4).

The Δ^{15}N value reflects the difference between individual host and symbiont δ^{15}N values and was assessed among species and depth ranges. Coral Δ^{15}N was highest in *L. hawaiiensis* (2.3 ± 1.2 ‰) and *L. scabra* (2.1 ± 0.6 ‰) and lowest in *L. glabra* (0.3 ± 1.1 ‰) and *C. levis* (0.5 ± 0.4 ‰) (Table 1; Figure 3B). The coral species had a significant effect on Δ^{15}N ($F_{4,21} = 3.490$, p = 0.025) with Tukey *post-hoc* tests revealing that *L. hawaiiensis* had significantly higher mean Δ^{15}N than *L. glabra* (+2 ‰) (t_{21} = -3.077, p = 0.041). There was no significant effect of irradiance level, with Δ^{15}N values remaining constant between corals from depths above and below 1% SI (1.4 – 1.5 ‰) ($F_{1,21}$ = 0.086, p = 0.773) (Table 1; Supplementary Table 4).

3.5 Trends in isotopic niches over species and irradiance levels

The isotopic niches of *L. glabra* and *L. hawaiiensis* hosts and symbionts did not overlap, with δ^{13}C values differentiating *L. glabra* isotopic niches while δ^{15}N values differentiated *L. hawaiiensis* niches. The isotopic niches of *P. speciosa* and *C. levis* showed slight overlap between hosts and symbionts. While there was insufficient data to plot isotopic niches of *L. scabra*, hosts and symbionts were also differentiated by δ^{15}N values (Figure 1C).
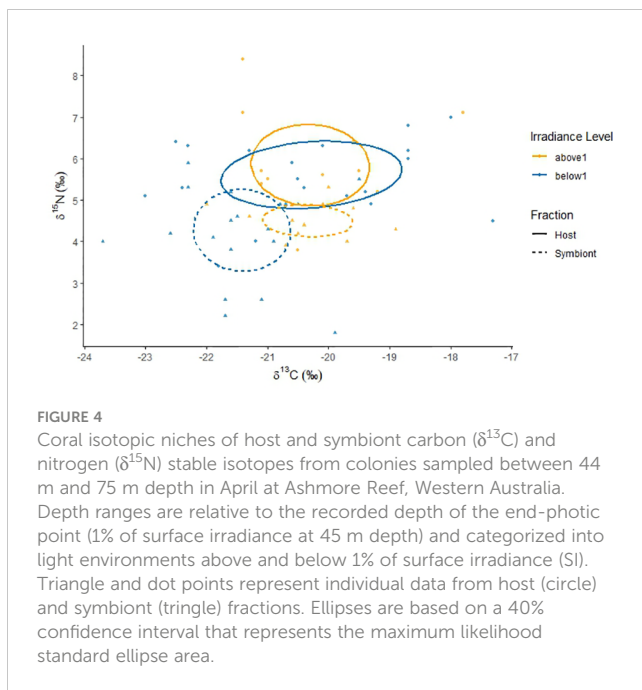
Isotopic niches of coral hosts and symbionts did not overlap at any irradiance level, with δ^{15}N values driving niche in corals at depths above 1% of surface irradiance, and ^{13}C and ^{15}N influencing differentiation in corals at depths below 1% of surface irradiance (Figure 4).

3.6 Host protein concentration

There was significant variance in protein among species ($F_{4,20} = 4.635$, p = 0.008), with *L. scabra* (2.26 ± 0.3 mg mL^{-1} cm^{-2}) and *C. levis* (1.9 ± 0.5 mg mL^{-1} cm^{-1}) having ~2 - 2.3 times higher protein concentrations than *P. speciosa* (0.97 ± 0.5 mg mL^{-1} cm^{-2}) (*L. scabra* vs. *P. speciosa*, t_{20} = 3.277, p = 0.028, and *C. levis* vs. *P. speciosa*, t_{20} = 3.515, p = 0.016) (Table 1; Supplementary Table 4), while *L. hawaiiensis* and *L. glabra* had similar protein concentrations of ~1.5 mg mL^{-1} cm^{-2} (Table 1). There were no correlations detected between protein concentration and depth (correlation = -0.094, t_{28} = 1.519, p = 0.140), and no statistical differences were detected in corals from depth above or below the end photic point (1% SI) ($F_{1,20}$ = 3.398, p = 0.080) (Table 1; Supplementary Table 4).

4 Discussion

To gain insight into the limits of acclimation of mesophotic corals, this study assessed autotrophy and heterotrophy through the analysis of SIA and protein concentrations of several mesophotic species at Ashmore Reef, Western Australia, across a 31 m depth

FIGURE 4
Coral isotopic niches of host and symbiont carbon (δ¹³C) and
nitrogen (δ¹⁵N) stable isotopes from colonies sampled between 44
m and 75 m depth in April at Ashmore Reef, Western Australia.
Depth ranges are relative to the recorded depth of the end-photic
point (1% of surface irradiance at 45 m depth) and categorized into
light environments above and below 1% of surface irradiance (SI).
Triangle and dot points represent individual data from host (circle)
and symbiont (tringle) fractions. Ellipses are based on a 40%
confidence interval that represents the maximum likelihood
standard ellipse area.

range (44 to 75 m) from light environments above and below the
end-photic point (at 1% of surface irradiance). We found that,
despite extremely low light conditions, *L. hawaiiensis*, *L. scabra*, and
P. speciosa were able to maintain metabolic processes
predominantly through photosynthetic carbon, whereas *L. glabra*
and *C. levis* showed higher dependencies on heterotrophy. No
significant differences between autotrophy and heterotrophy were
observed between corals from depths above versus below 1% of
surface irradiance and thus, the end-photic point does not represent
an environmental threshold for nutrient acquisition in this study.
This research presents the first physiological data for *C. levis*
(observed 44 – 75 m), an understudied and apparently
uncommon depth-specialist species.

4.1 Varying carbon sources among species

The lowest host δ¹³C value was -23.0 ‰ in our study (*L.
hawaiiensis*), with an even lower symbiont δ¹³C value of -23.7 ‰
(different colony of *L. hawaiiensis*) that may be the lowest reported
for a symbiotic scleractinian coral, thus expanding recorded δ¹³C
ranges. Similarly low host and symbiont δ¹³C values were reported
for mesophotic coral in Hawaii (-22.7 ‰), Red Sea (-22.7 ‰), and
Jamaica (-22.4 ‰) (Muscatine et al., 1989; Einbinder et al., 2009;
Padilla-Gamiño et al., 2019), providing insight into the metabolic
limits of corals. In general, symbiont δ¹³C values tended to be more
negative than host δ¹³C in our study. It is likely that metabolic CO_2
derived from mesophotic hosts with low δ¹³C may drive the
particularly low symbiont δ¹³C values observed, in addition to
greater isotopic discrimination due to reduced photosynthesis
(Muscatine et al., 1989). This trend could also be attributed to a
higher concentration of ¹³C-depleted fatty tissues (*e.g.*, lipids)
(Alamaru et al., 2009; Sturaro et al., 2019), which can be

considerably elevated in symbiont cells compared to their host
(Radice et al., 2019a).

Increasingly negative symbiont δ¹³C over depth indicated that
photosynthetic activity was reduced as light availability decreased
(Farquhar et al., 1989; Muscatine et al., 1989; Lesser et al., 2022).
Despite this, *L. hawaiiensis*, *P. speciosa* and *L. scabra* had Δ¹³C
values close to zero, suggesting reliance on symbiont-derived
carbon and efficient carbon cycling (Muscatine et al., 1989).
Pachyseris speciosa is primarily more autotrophic (Veron, 2000)
and does not increase heterotrophy over depth in another Indian
Ocean location (Radice et al., 2019a; Radice et al., 2019b; Radice
et al., 2022), thus this species provides good indication that δ¹³C
interpretations of autotrophy in this study are robust.

In contrast, *L. glabra* and *C. levis* had higher distinctions between
their host and symbiont δ¹³C (Δ¹³C = 1.4 ± 1 ‰ and 3.5 ± 1.7 ‰,
respectively), indicating greater assimilations of externally-derived
nutrients, likely in compensation for low photosynthetic carbon
assimilation (Swart, 1983; Reynaud et al., 2002; Palardy et al., 2008;
Lesser et al., 2010). Host δ¹³C of these species were also within the
ranges of small plankton (-17 ‰ to -21 ‰) (Land et al., 1975;
Fontugne and Claude Duplessy, 1978; Rodrigues and Grottoli, 2006).
The capacity for heterotrophic prey uptake is species-specific and
subject to food availability (Ferrier-Pagès et al., 2003; Tremblay et al.,
2015). High chlorophyll-*a* concentrations at the sampling depths
(~1.5 mg m⁻³) suggest rich availability of particulate matter in the
mesophotic at Ashmore Reef (*i.e.*, phytoplankton) that would
support zooplankton (Kiørboe, 2011), particularly compared to
other mesophotic ecosystems (*e.g.*, 0.6 - 1 mg m⁻³) (Bridge et al.,
2011; Ziegler et al., 2015). Thus, it is likely that corals in this oceanic
reef are acquiring higher levels of plankton to meet metabolic
demands. The mixotrophic abilities of scleractinian zooxanthellate
corals, however, comprise a range across a spectrum. Clear separation
of *L. glabra* isotopic niches driven by δ¹³C suggest the reliance for
heterotrophy in this species exceeds that of *C. levis*, which shows
slight overlap.

4.2 Higher Δ¹⁵N in autotrophic vs. heterotrophic reliant species

Nitrogen is essential for maintaining symbiont growth,
photosynthesis and overall holobiont health in corals (Falkowski
et al., 1993; Radecker et al., 2015). Lower Δ¹⁵N values were recorded
in corals exhibiting greater heterotrophic inputs of carbon (*L. glabra*,
C. levis) compared to corals assimilating more photosynthates
(*L. hawaiiensis*, *P. speciosa*, *L. scabra*). In typical food webs,
consumers exhibit a stepwise enrichment of δ¹⁵N and as such, can
be used to determine trophic position (Minagawa and Wada, 1984;
Lesser et al., 2010). If applying this method to corals, we would expect
the host tissues to have significantly higher δ¹⁵N than its symbiont.
Yet, the effects of acquiring nitrogen from multiple sources (Mullin
et al., 1984) and effective nitrogen recycling within the holobiont
(Reynaud et al., 2009; Tremblay et al., 2015; Rangel et al., 2019)
complicates the application of a coral trophic enrichment factor that
is likely lower (0 - 2 ‰) than in other animals (Radice et al., 2022).

In addition to particulate matter capture, corals obtain nitrogen through the uptake of dissolved inorganic nitrogen (DIN) in the forms of ammonium and nitrate (Mullin et al., 1984; Grover et al., 2002). Ammonium is preferred by corals (Bythell, 1990), however, nitrate often increases in availability from shallow to mesophotic depths (Mullin et al., 1984; Morrow et al., 2016; Radice et al., 2021). Ammonium is depleted in ^{15}N (Miyake and Wada, 1967), thus it would be expected that its acquisition decreases coral δ^{15}N. The δ^{15}N of nitrate is generally correlated to its concentration levels (Erler et al., 2015; Isaji et al., 2022), but deep-water nitrate typically fall between ~5 – 7 ‰ at subsurface depths (< 200 m) because of the deep-water oceanic pool (Sigman et al., 2009; Sigman and Fripiat, 2019; Isaji et al., 2022). When considering that (1) DIN is mostly acquired and used by the symbionts (Muscatine and D'Elia, 1978; Pernice et al., 2012), and (2) the uptake rates of ammonium can be significantly higher in more autotrophic vs. more heterotrophic corals (Grover et al., 2002) - the acquisition of both dissolved inorganic nitrate and ammonium can explain higher host vs. symbiont δ^{15}N values in photosynthate-dependent corals (*L. hawaiiensis*, *P. speciosa* and *L. scabra*) (Δ^{15}N =1.2 to 2.3 ‰).

By contrast, the very similar host and symbiont δ^{15}N values in *L. glabra* and *C. levis* demonstrate tight holobiont nitrogen recycling (Δ^{15}N = 0.3 - 0.5 ‰) (Reynaud et al., 2009; Rangel et al., 2019), with Δ^{15}N differences being significant between *L. glabra* (more heterotrophic) and *L. hawaiiensis* (more autotrophic). Nitrogen can be translocated between the host and symbiont within hours (Tremblay et al., 2015), which may become particularly important if light limitation affects symbiont nitrogen uptake. As plankton ingestion can result in the synthesis of over three times more nitrogen than DIN (Hoegh-Guldberg and Williamson, 1999; Grover et al., 2002), it is hypothesized that heterotrophic nitrogen acquisition from plankton or particulate organic matter could provide a metabolic advantage to the uptake of dissolved nitrogen. If symbiont density decreases over depth (Ziegler et al., 2015) with lower photosynthate reliance, this may in turn reduce overall nitrogen needs, allowing the recycling process of heterotrophically-derived nitrogen (Ferrier-Pagès et al., 2021) to meet overall holobiont demands (as seen in *L. glabra* and *C. levis* in this study). Interestingly, *L. hawaiiensis* and *L. scabra* may increase symbiont density over depth (Padilla-Gamiño et al., 2019). This could further explain why the more autotrophic-dependent species in our study exhibited less efficient nitrogen recycling likely due to reliance on DIN to meet higher nitrogen demands, which has a high turnover in coral cells (Krueger et al., 2018), and may be less effective metabolically (Hoegh-Guldberg and Williamson, 1999; Grover et al., 2002).

4.3 Challenges in interpreting trophic strategies in mesophotic corals with stable isotopes

Our analysis has highlighted some constraints in understanding trophic ecology in mesophotic corals using common techniques used for interpreting δ^{13}C and δ^{15}N. The correlations seen in this study between host and symbiont Δ^{13}C and Δ^{15}N were not analogous. In other studies, corals that have exhibited very similar host and symbiont δ^{13}C (*i.e.*, reliant on photosynthates - Peterson and Fry, 1987; Muscatine et al., 1989), have also displayed differentiated δ^{15}N values. For example, *Porites evermanni* (Δ^{13}C = -0.13 ± 0.47 ‰ and Δ^{15}N = -1.79 ± 0.68 ‰) (Price et al., 2021), *Platygyra* spp., (Δ^{13}C = -0.70 ± 0.46 ‰ and Δ^{15}N = 2.50 ± 1.20 ‰), *Favites* spp., (Δ^{13}C = -0.50 ± 0.52 ‰ and Δ^{15}N = 2.50 ± 1.39 ‰) (Conti-Jerpe et al., 2020), and *Montastraea cavernosa* that has an isotopic niche differentiation driven by Δ^{15}N but not Δ^{13}C at mesophotic depths (Lesser et al., 2022). Yet, these particular metrics (Δ^{13}C values close to 0, and higher Δ^{15}N values) are generally considered evidence of increasing heterotrophy (*e.g.*, Conti-Jerpe et al., 2020; Price et al., 2021).

Furthermore, Δ^{15}N values close to zero have also been recorded in species with larger Δ^{13}C (*i.e.*, Δ^{13}C values that indicate external carbon acquisition), such as *Montipora capitata* where Δ^{13}C = 1.53 ± 0.63 and Δ^{15}N = 0.09 ± 0.50 ‰ (Price et al., 2021), and *Stylophora pistillata* whereby its isotopic niche differentiation was driven by Δ^{13}C but not by Δ^{15}N at mesophotic depths (Lesser et al., 2022). Yet, these metrics (higher Δ^{13}C with lower Δ^{15}N) are commonly assessed to be primarily autotrophic (*e.g.*, Price et al., 2021).

The methods used to interpret stable isotope data in the context of coral trophic ecology include (1) calculating the differences between host and symbiont δ^{13}C (Δ^{13}C or δ^{13}C$_{host-symbionts}$), whereby a more negative value is said to indicate greater heterotrophic contribution (Muscatine et al., 1989; Price et al., 2021), (2) calculating the differences between host and symbiont δ^{15}N (Δ^{15}N or δ^{15}N$_{host-symbionts}$), where by higher values denote heterotrophy) (*e.g.*, Conti-Jerpe et al., 2020; Price et al., 2021; Lesser et al., 2022) and (3) SIBER Bayesian models, whereby a greater differentiation in isotopic niches of δ^{13}C and δ^{15}N indicate greater heterotrophic reliance (Jackson et al., 2011; Conti-Jerpe et al., 2020).

The Δ^{13}C metric does not appear to work the same for corals in low light environments such as in our study. This metric relies on the coral host becoming more depleted in δ^{13}C due to external carbon sources being more depleted in δ^{13}C than the coral host and symbiont. This is typically true for corals in shallow light environments and even many mesophotic environments. Yet, under a more extreme light condition, symbiont δ^{13}C can be extremely negative (*e.g.*, this study, -22 to -23 ‰), and external food sources, such as plankton and particulate matter, could likely be more enriched than the photosynthetic carbon source (*i.e.*, the symbiont) (Land et al., 1975; Fontugne and Claude Duplessy, 1978; Rodrigues and Grottoli, 2006) although plankton was not assessed in our study. Alternatively, for mesophotic corals, Δ^{13}C values that deviate from zero may denote a significant input of carbon sources external to the holobiont, despite whether Δ^{13}C is, for example, +2 ‰ vs. -2 ‰.

The Δ^{15}N metric relies on the stepwise process of δ^{15}N enrichment in the coral host consumer (Minagawa and Wada, 1984), much like the latter approach (SIBER), where differentiation in coral host and symbiont isotopic niches can be driven individually by δ^{15}N (with little δ^{13}C differentiation) and be labelled as heterotrophic. The fact that corals assimilate DIN (which can vary in δ^{15}N), and also recycle both heterotrophic and

autotrophic nitrogen within the holobiont, makes this metric particularly challenging to assess. In addition, a recent re-analysis of pooled data from previously published studies (Lesser et al., 2022) found no overall trends between $\delta^{15}N$ and heterotrophy in mesophotic corals, and also symbiont type can influence DIN assimilation in relation to light availability (Ezzat et al., 2017). Thus, we argue that using $\delta^{15}N$ as an indication of heterotrophy is not consistent across coral species and depths, particularly in mesophotic environments, and $\delta^{13}C$ appears to be the primary determinant of mixotrophy in these ecosystems.

4.4 Species-specific protein concentrations

Protein concentration often decreases over depth in autotrophic corals (Cooper et al., 2011a; Ziegler et al., 2015), yet the capacity for heterotrophic carbon to promote tissue generation (Krueger et al., 2018) and higher protein levels (Grover et al., 2002; Houlbrèque et al., 2004; Rodrigues and Grottoli, 2006; Reynaud et al., 2009; Hoogenboom et al., 2015) suggests heterotrophic feeding at depth could benefit overall tissue protein and biomass. However, our coral samples were from much lower irradiances than other similar studies and protein concentrations showed no obvious patterns in relation to trophic strategy.

The trends we observed were consistent with species-specific protein concentrations observed by Brunner, 2015 where *Leptoseris scabra* had significantly higher host tissue protein concentrations than *P. speciosa*, despite both having similar nutrient acquisition strategies. Over depth, *P. speciosa* maintains a single symbiont genus (*Cladocopium*) with reduced photosynthetic energy (Cooper et al., 2011a), typically accompanied by reductions in tissue biomass (Cooper et al., 2011a; Brunner, 2015) and symbiont density (Brunner, 2015). By contrast, *L. scabra* shows the ability to maintain relatively high protein concentrations, likely as a result of specialized physiological adaptations (Brunner, 2015; Pochon et al., 2015; Padilla-Gamiño et al., 2019) and highlights the acclimatory mechanisms depth-specialists use to maximize the use of nutrients available at depth. Interestingly, all *Leptoseris* species examined herein do not significantly decrease protein concentrations with depth (Brunner, 2015). For example, at 80 m in the Coral Sea, *P. speciosa* had protein concentrations of approximately 0.9 mg cm^2 (following continual decline), compared to *L. scabra* (1.25 mg cm^2), even though *L. hawaiiensis* had less protein at this depth (0.75 mg cm^2) than *P. speciosa* (Brunner, 2015) (*i.e.*, a much brighter light environment than this study). Given this, it is likely that the low protein values reported in this study reflect reducing protein synthesis capabilities for *P. speciosa* at end-photic irradiances (Cooper et al., 2011a; Brunner, 2015).

4.5 Species-specific potential in a light limited environment

The light environment at Ashmore Reef attenuated strongly (1% at 54 m, PAR$_{kd}$ = 0.069 m^{-1}) compared to other regions such as

Bermuda and the Bahamas, where the same light availability occurs at 100 m and 81 m, respectively (Fricke et al., 1987; Lesser et al., 2010). This likely reflects the rich phytoplankton abundances present in the highly productive mesophotic ecosystems at Ashmore Reef (Kiørboe, 2011; Kahng et al., 2019). Similar end-photic depths have been observed in other highly productive systems such as the Maldives, where only 4% of surface irradiance was measured at 30 m (Radice et al., 2019a).

Our results build on information that implies *P. speciosa* is an obligate autotroph with restricted trophic plasticity over depth (Radice et al., 2019a; Radice et al., 2019b; Radice et al., 2022). This likely limits the depth distribution in this species and the fact that colonies were only found shallower than 60 m supports the notion of *P. speciosa* as a depth-generalist coral (Chow et al., 2019). Other studies also found *P. speciosa* typically at 60 m and shallower, with deeper observations only occurring in MCEs with exceptionally low light attenuation (*e.g.*, the Coral Sea and French Polynesia) (Englebert et al., 2014; Pichon, 2019; Bongaerts et al., 2021). In contrast, the irradiance level at 60 m at Ashmore Reef is equivalent to light conditions beyond the photic point (1% SI) (*i.e.*, deeper than 60 m at other locations), which suggests that *P. speciosa* may be capable of inhabiting lower mesophotic depths at other locations. The ability for this species to remain primarily autotrophic in such extreme light conditions is likely permitted through significantly reduced tissue mass and symbiont density (Brunner, 2015) and possibly specialized intracellular arrangements (*i.e.*, monolayer to reduce shading) (Schlichter et al., 1986; Kahng et al., 2019) that allow it to acclimatize to lower photosynthate assimilation.

The variation in carbon and nitrogen sources was most distinct between *L. hawaiiensis* and *L. glabra* (significantly different $\Delta^{13}C$ and symbiont $\Delta^{15}N$), highlighting the species-specific occupation of different ecological niches despite living in the same environments. *Leptoseris* species are specialized to inhabit light environments approaching photic limits and can maintain metabolic demands via heterotrophy at these low irradiances (Fricke et al., 1987; Padilla-Gamiño et al., 2019), as demonstrated by *L. glabra* in this study. Research by Padilla-Gamiño et al. (2019) highlighted differences in physiological adaptations between *Leptoseris* species also examined in this study, whereby *L. scabra* increased photosynthetic pigments with depth while *L. hawaiiensis* employed high pigment content across low symbiont densities. Symbiont type can influence photo-adaptation (Ziegler et al., 2015; Padilla-Gamiño et al., 2019) and symbiont plasticity demonstrated by *Leptoseris* spp. in other studies and could indicate photoautotrophic benefits over depth (Cooper et al., 2011a; Padilla-Gamiño et al., 2019; Martinez et al., 2020), compared to *P. speciosa* which maintains one symbiont genus over depth with reduced photosynthetic productivity (Cooper et al., 2011b; Ziegler et al., 2015). These adaptations likely enable *L. scabra* and *L. hawaiiensis* to maintain higher protein contents at depth without significant heterotrophic input, compared to the *P. speciosa*. Further studies are required to assess the specific physiological adaptations among mesophotic species at Ashmore Reef. This study provides the first assessment of trophic ecology in *L. glabra* and *C. levis*, hence no comparative data are available for assessing photosynthetic capacity in these species.

5 Conclusions

This study provides new insight into the ecophysiology of mesophotic corals in the Eastern Indian Ocean region. The finding that this system has relatively shallow photic end points possibly due to a high level of productivity provides an interesting contrast to other mesophotic systems in Australia such as the Coral Sea. Both depth-specialist and depth-generalist corals demonstrated the ability to remain photosynthetically reliant in just a fraction of surface irradiance. The role of nitrogen recycling in the coral holobiont is not fully understood, particularly between different trophic strategies in limited light environments, and this research provides interesting insight into potential links between heterotrophically-derived nitrogenous benefits and species-specific nitrogen demands at depth. Nevertheless, further studies are required to broaden the understanding of nutrient acquisition and allocation in mesophotic corals, and deeper investigations into how external sources and internal processes influence $\delta^{15}N$ under autotrophic and heterotrophic reliance in low light is warranted.

Overall, this study highlights the remarkable capacity of mesophotic Scleractinia to optimize their physiology in light limited environments and provides insight into potential acclimation limits for depth specialist and generalist species. Additionally, this is the first investigation of nutrient acquisition or protein content in *C. levis* and demonstrates its requirement to obtain nutrients mixotrophically in low light environments. These findings contribute to the narrow yet growing pool of literature on mesophotic coral ecophysiology and underscore the need for further research that betters our understanding of how various nutrient inputs affect coral physiology and stable isotopes $\delta^{13}C$ and $\delta^{15}N$ at depth.

Data availability statement

The raw data supporting the conclusions of this article will be made available by the authors, without undue reservation.

Author contributions

ZR and KMi conceived the project and secured funding. AC, VR, ZR, and KMc conducted experimental and analytical design. AC conducted the field work and KMi was the Chief Scientist on the field expedition. AC and AH carried out laboratory work. ZR performed all coral taxonomy. AC and VR performed statistical analyses and drafted the manuscript. All authors conducted manuscript edits. All authors contributed to the article and approved the submitted version.

Conflict of interest

The authors declare that the research was conducted in the absence of any commercial or financial relationships that could be construed as a potential conflict of interest.

Publisher's note

All claims expressed in this article are solely those of the authors and do not necessarily represent those of their affiliated organizations, or those of the publisher, the editors and the reviewers. Any product that may be evaluated in this article, or claim that may be made by its manufacturer, is not guaranteed or endorsed by the publisher.

Supplementary material

The Supplementary Material for this article can be found online at: https://www.frontiersin.org/articles/10.3389/fmars.2023.1089746/full#supplementary-material

References

Alamaru, A., Loya, Y., Brokovich, E., Yamd, R., and Shemesh, A. (2009). Carbon and nitrogen utilization in two species of red Sea corals along a depth gradient: insights from stable isotope analysis of total organic material and lipids. *Geochimica Cosmochimica Acta* 73, 5333–5342. doi: 10.1016/j.gca.2009.06.018

Anthony, K. R. N., and Fabricius, K. E. (2000). Shifting roles of heterotrophy and autotrophy in coral energetics under varying turbidity. *J. Exp. Mar. Biol. Ecol.* 252, 221–253. doi: 10.1016/S0022-0981(00)00237-9

Armstrong, R. A., Pizarro, O., and Roman, C. (2019). "Underwater robotic technology for imaging mesophotic coral ecosystems," in *Mesophotic coral ecosystems. coral reefs of the world.* Eds. Y. Loya, K. Puglise and T. Bridge (Cham: Springer).

Arrigoni, R., Berumen, M. L., Stolarski, J., Terraneo, T. I., and Benzoni, F. (2019). Uncovering hidden coral diversity: a new cryptic lobophylliid scleractinian from the Indian ocean. *Cladistics* 35, 301–328. doi: 10.1111/cla.12346

Baker, A. C. (2003). Flexibility and specificity coral-algal symbiosis: diversity, ecology, and biogeography of symbiodinium. *Annu. Rev. Ecology Evolution Systematics* 34, 661–689. doi: 10.1146/annurev.ecolsys.34.011802.132417

Ben-David, M., and Flaherty, E. A. (2012). Stable isotopes in mammalian research: a beginner's guide. *J. Mammalogy* 92, 312–328. doi: 10.1644/11-MAMM-S-166.1

Benzoni, F., Arrigoni, R., Stefani, F., and Stolarski, J. (2012). Systematics of the coral genus *Craterastrea* (Cnidaria, anthozoa, scleractinia) and description of a new family through combined morphological and molecular analyses. *Systematics Biodiver.* 10, 417–433. doi: 10.1080/14772000.2012.744369

Bhagooli, R., Mattan-Moorgawa, S., Kaullysing, D., Louis, Y. D., Gopeechund, A., Ramah, S., et al. (2021). Chlorophyll fluorescence – a tool to assess photosynthetic performance and stress photophysiology in symbiotic marine invertebrates and seaplants. *Mar. pollut. Bull.* 165, 112059–112059. doi: 10.1016/j.marpolbul.2021.112059

Bongaerts, P., Cooke, I. R., Ying, H., Wels, D., Haan Den, S., Hernandez-Agreda, A., et al. (2021). Morphological stasis masks ecologically divergent coral species on tropical reefs. *Curr. Biol.* 31, 2286–2298.e8. doi: 10.1016/j.cub.2021.03.028

Bongaerts, P., Frade, P. R., Hay, K. B., Englebert, N., Latijnhouwers, K. R. W., Bak, R. P. M., et al. (2015). Deep down on a Caribbean reef: lower mesophotic depths harbor a specialized coral-endosymbiont community. *Sci. Rep.* 5 (1), 7652. doi: 10.1038/srep07652

Bongaerts, P., and Smith, T. B. (2019). "Beyond the "Deep reef refuge" hypothesis: a conceptual framework to characterize persistence at depth," in *Mesophotic coral ecosystems. coral reefs of the world.* Eds. Y. Loya, K. Puglise and T. Bridge (Cham: Springer Nature).

Brakel, W. H. (1979). Small-scale spatial variation in light available to coral reef benthis: quantum irradiance measurements from a Jamaican reef. *Bull. Mar. Sci.* 29, 406–413.

Bridge, T. C. L., Done, T. J., Beaman, R. J., Friedman, A., Williams, S. B., Pizarro, O., et al. (2011). Topography, substratum and benthic macrofaunal relationships on a tropical mesophotic shelf margin, central great barrier reef, Australia. *Coral Reefs* 30, 143–153. doi: 10.1007/s00338-010-0677-3

Brunner, C. A. (2015). *Physiological adaptations of mesophotic corals across a depth gradient – leptoseris spp. & pachyseris speciosa (Scleractinia: agariciidae)* (Bremen, Germany: Universität Bremen).

Bythell, J. C. (1990). Nutrient uptake in the reef-building coral *Acropora palmata* at natural environmental concentrations. *Mar. Ecol. Prog. Ser.* 68, 65–69. doi: 10.3354/meps068065

Chow, G. S. E., Chan, Y. K. S., Jain, S. S., and Huang, D. (2019). Light limitation selects for depth generalists in urbanised reef coral communities. *Mar. Environ. Res.* 147, 101–112. doi: 10.1016/j.marenvres.2019.04.010

Conti-Jerpe, I. E., Thompson, P. D., Wong, C. W. M., Oliveira, N. L., Duprey, N. N., Moynihan, M. A., et al. (2020). Trophic strategy and bleaching resistance in reef-building corals. *Sci. Adv.* 6, eaaz5443–eaaz5443. doi: 10.1126/sciadv.aaz5443

Cooper, T. F., Karin, E. U., Sana, S. D., Andrew, J. H., Michael, K., Andrew, M., et al. (2011a). Niche specialization of reef-building corals in the mesophotic zone: metabolic trade-offs between divergent symbiodinium types. *Proc. Biol. Sci.* 278, 1840–1850. doi: 10.1098/rspb.2010.2321

Cooper, T. F., Lai, M., Ulstrup, K. E., Saunders, S. M., Flematti, G. R., Radford, B., et al. (2011b). Symbiodinium genotypic and environmental controls on lipids in reef building corals. *PLoS One* 6, e20434. doi: 10.1371/journal.pone.0020434

Coplen, T. B. (2011). Guidelines and recommended terms for expression of stable-isotope-ratio and gas-ratio measurement results. *Rapid Commun. Mass Spectrometry* 25, 2538–2560. doi: 10.1002/rcm.5129

Coplen, T. B., Brand, W. A., Gehre, M., Gröning, M., Meijer, H. A. J., Toman, B., et al. (2006). New guidelines for $\delta^{13}C$ measurements. *Analytical Chem.* 78, 2439–2441. doi: 10.1021/ac052027c

Crandall, J. B., Teece, M. A., Estes, B. A., Manfrino, C., and Ciesla, J. H. (2016). Nutrient acquisition strategies in mesophotic hard corals using compound specific stable isotope analysis of sterols. *J. Exp. Mar. Biol. Ecol.* 474, 133–141. doi: 10.1016/j.jembe.2015.10.010

Dinesen, Z. D. (1980). A revision of the coral genus *Leptoseris* (Scleractinia: fungiia: agariciidae). *Mem Queens Mus* 20, 181–235. Available at: https://biostor.org/reference/151870.

Einbinder, S., Mass, T., Brokovich, E., Dubinsky, Z., Erez, J., and Tchernov, D. (2009). Changes in morphology and diet of the coral *Stylophora pistillata* along a depth gradient. *Mar. Ecol. Prog. Ser.* 381, 167–174. doi: 10.3354/meps07908

Englebert, N., Bongaerts, P., Muir, P., Hay, K. B., and Hoegh-Gulberg, O. (2014). Deepest zooxanthellate corals of the great barrier reef and coral Sea. *Mar. Biodiver.* 45, 1–2. doi: 10.1007/s12526-014-0221-8

Englebert, N., Bongaerts, P., Muir, P. R., Hay, K. B., Pichon, M., and Hoegh-Guldberg, O. (2017). Lower mesophotic coral communities (60-125m depth) of the northern great barrier reef and coral Sea. *PLoS One* 12, e0170336. doi: 10.1371/journal.pone.0170336

Erler, D. V., Wang, X. T., Sigman, D. M., Scheffers, S. R., and Shepherd, B. O. (2015). Controls on the nitrogen isotopic composition of shallow water corals across a tropical reef flat transect. *Coral Reefs* 24, 329–338. doi: 10.1007/s00338-014-1215-5

Eyal, G., Laverick, J. H., Bongaerts, P., Levy, O., and Pandolfi, J. M. (2021). Mesophotic coral ecosystems of the great barrier reef are understudied and underexplored. *Front. Mar. Sci.* 8, 622856. doi: 10.3389/fmars.2021.622856.

Ezzat, L., Fine, M., Grover, R., and Ferrier-Pagés, C. (2017). Carbon and nitrogen acquisition in shallow and deep holobionts of the scleractinian coral *S. pistillata*. *Front. Mar. Sci.* 4. doi: 10.3389/fmars.2017.00102

Falkowski, P. G., Dubinsky, Z., Muscatine, L., and Mccloskey, L. (1993). Population control in symbiotic corals. *BioScience* 43, 606–611. doi: 10.2307/1312147

Farquhar, G. D., Ehleringer, J. R., and Hubick, K. T. (1989). Carbon isotope discrimination and photosynthesis. *Annu. Rev. Plant Physiol. Plant Mol. Biol.* 40, 503–537. doi: 10.1146/annurev.pp.40.060189.002443

Ferrier-Pagés, C., Bednarz, V., Grover, R., Benayahu, Y., Maguer, J. F., Rottier, C., et al. (2021). Symbiotic stony and soft corals: is their host-algae relationship really mutualistic at lower mesophotic reefs? *Limnology Oceanogr.* 67, 261–271. doi: 10.1002/lno.11990

Ferrier-Pagés, C., Peirano, A., Abbate, M., Cocito, S., Negri, A., Rottier, C., et al. (2011). Summer autotrophy and winter heterotrophy in the temperate symbiotic coral *Cladocora caespitosa*. *Limnology Oceanogr.* 56, 1429–1438. doi: 10.4319/lo.2011.56.4.1429

Ferrier-Pagés, C., Witting, J., Tambutté, E., and Sebens, K. P. (2003). Effect of natural zooplankton feeding on the tissue and skeletal growth of the scleractinian coral *Stylophora pistillata*. *Coral Reefs* 22, 229–240. doi: 10.1007/s00338-003-0312-7

Fontugne, M., and Claude Duplessy, J. (1978). Carbon isotope ratio of marine plankton related to surface water masses. *Earth Planetary Sci. Lett.* 41, 365–371. doi: 10.1016/0012-821X(78)90191-7

Fricke, H. W., Vareschi, E., and Schlichter, D. (1987). Photoecology of the coral *Leptoseris fragilis* in the red Sea twilight zone (an experimental study by submersible). *Oecologia* 73, 371–381. doi: 10.1007/BF00385253

Genty, B., Briantais, J.-M., and Baker, N. R. (1989). The relationship between the quantum yield of photosynthetic electron transport and quenching of chlorophyll fluorescence. *Biochim. Biophys. Acta (BBA) - Gen. Subj.* 990, 87–92. doi: 10.1016/S0304-4165(89)80016-9

Gilmour, J. P., Cook, K. L., Ryan, N. M., Puotinen, M. L., Green, R. H., Shedrawi, G., et al. (2019). The state of Western australia's coral reefs. *Coral Reefs* 38, 651–667. doi: 10.1007/s00338-019-01795-8

Glynn, P. W. (1996). Coral reef bleaching: facts, hypotheses and implications. *Global Change Biol.* 2, 495–509. doi: 10.1111/j.1365-2486.1996.tb00063.x

Grover, R., Maguer, J.-F., Reynaud-Vaganay, S., and Ferrier-Pagès, C. (2002). Uptake of ammonium by the scleractinian coral *Stylophora pistillata*: effect of feeding, light, and ammonium concentrations. *Limnology Oceanogr.* 47, 782–790. doi: 10.4319/lo.2002.47.3.0782

Heikoop, J. M., Dunn, J., Risk, M. J., Sanderman, I. M., Schwarcz, H., and Waltho, N. (1998). Relationship between light and the $\delta^{15}N$ of coral tissue: examples from Jamaica and Zanzibar. *Limnology Oceanogr.* 43, 909–920. doi: 10.4319/lo.1998.43.5.0909

Heyward, A., and Radford, B. (2019). "Northwest Australia," in *Mesophotic coral ecosystems.* Eds. Y. Loya, K. Puglise and T. Bridge (Cham: Springer).

Hoegh-Guldberg, O. (1988). A method for determining the surface area of corals. *Coral Reefs* 7, 113–116. doi: 10.1007/BF00300970

Hoegh-Guldberg, O., and Williamson, J. (1999). Availability of two forms of dissolved nitrogen to the coral *Pocillopora damicornis* and its symbiotic zooxanthellae. *Mar. Biol.* 133, 561–570. doi: 10.1007/s002270050496

Hoeksema, B. W., Bongaerts, P., and Baldwin, C. C. (2017). High coral cover at lower mesophotic depths: a dense *Agaricia* community at the leeward side of curaçao, Dutch Caribbean. *Mar. Biodiver.* 47, 67–70. doi: 10.1007/s12526-015-0431-8

Hoogenboom, M., Rottier, C., Sikorski, S., and Ferrier-Pagés, C. (2015). Among-species variation in the energy budgets of reef-building corals: scaling from coral polyps to communities. *J. Exp. Biol.* 218, 3866–3877. doi: 10.1242/jeb.124396

Houlbrèque, F., and Ferrier-Pagès, C. (2009). Heterotrophy in tropical scleractinian corals. *Biolovical Rev.* 84, 1–17. doi: 10.1111/j.1469-185X.2008.00058.x

Houlbrèque, F., Tambutte, E., and Ferrier-Pagès, C. (2003). Effect of zooplankton availability on the rates of photosynthesis, and tissue and skeletal growth in the

scleractinian coral *Stylophora pistillata*. *J. Exp. Mar. Biol. Ecol.* 292, 145–166. doi: 10.1016/S0022-0981(03)00259-4

Houlbrèque, F., Tambutté, E., Allemand, D., and Ferrier-Pagès, C. (2004). Interactions between zooplankton feeding, photosynthesis and skeletal growth in the scleractinian coral *Stylophora pistillata*. *J. Exp. Biol.* 207, 1461–1469. doi: 10.1242/jeb.00911

Isaji, Y., Yoshikawa, C., Ogawa, N. O., Matsumoto, K., Makabe, A., Toyoda, S., et al. (2022). Nitrogen sources for phytoplankton in the Eastern Indian ocean determined from $\delta^{15}N$ of chlorophyll a and divinyl chlorophyll a. *Geochem. Geophysics Geosystems* 23, e2021GC010057. doi: 10.1029/2021GC010057

Jackson, A. L., Inger, R., Parnell, A. C., and Bearhop, S. (2011). Comparing isotopic niche widths among and within communities: SIBER – stable isotope Bayesian ellipses in R. *J. Anim. Ecol.* 80, 595–602. doi: 10.1111/j.1365-2656.2011.01806.x

Kahng, S. E., Akkaynak, D., Shlesinger, T., Hochberg, E. J., Wiedenmann, J., Tamir, R., et al. (2019). "Light, temperature, photosynthesis, heterotrophy, and the lower depth limits of mesophotic coral ecosystems," in *Mesophotic coral ecosystems* (Cham: Springer International Publishing).

Kahng, S. E., Copus, J. M., and Wagner, D. (2014). Recent advances in the ecology of mesophotic coral ecosystems (MCEs). *Curr. Opin. Environ. Sustainability* 7, 71–81. doi: 10.1016/j.cosust.2013.11.019

Kiørboe, T. (2011). How zooplankton feed: mechanisms, traits and trade-offs. *Biol. Rev.* 86, 311–339. doi: 10.1111/j.1469-185X.2010.00148.x

Kirk, J. T. O. (2011). *Light and photosynthesis in aquatic ecosystems. 3rd ed* (New York: Cambridge University Press).

Krueger, T., Bodin, J., Horwitz, N., Loussert-Fonta, C., Sakr, A., Escrig, S., et al. (2018). Temperature and feeding induce tissue level changes in autotrophic and heterotrophic nutrient allocation in the coral symbiosis – a NanoSIMS study. *Sci. Rep.* 8, 12710. doi: 10.1038/s41598-018-31094-1

Land, L. S., Lang, J. C., and Smith, B. C. (1975). Preliminary observations on the carbon isotopic composition of some reef coral tissues and symbiotic zooxanthellae. *Limnology Oceanogr.* 20, 283–287. doi: 10.4319/lo.1975.20.2.0283

Laverick, J. H., Piango, S., Andradi-Brown, D. A., Exton, D. A., Bongaerts, P., Bridge, T. C. L., et al. (2018). To what extent do mesophotic coral ecosystems and shallow reefs share species of conservation interest? a systematic review. *Environ. Evidence* 7, 15. doi: 10.1186/s13750-018-0127-1

Lesser, M. P., Falcón, L. I., Rodríguez-Román, A., Enríquez, S., Hoegh-Guldberg, O., and Iglesias-Prieto, R. (2007). Nitrogen fixation by symbiotic cyanobacteria provides a source of nitrogen for the scleractinian coral montastraea cavernosa. *Mar. Ecol. Prog. Ser.* 346, 143–152. doi: 10.3354/meps07008

Lesser, M. P., Slattery, M., Laverick, J. H., Macartney, K. J., and Bridge, T. C. (2019). Global community breaks at 60 m on mesophotic coral reefs. *Global Ecol. Biogeogr.* 28, 1403–1416. doi: 10.1111/geb.12940

Lesser, M. P., Slattery, M., and Macartney, K. J. (2022). Using stable isotope analyses to assess the trophic ecology of scleractinian corals. *Oceans* 3, 527–546. doi: 10.3390/oceans3040035

Lesser, M. P., Slattery, M., Stat, M., Ojimi, M., Gates, R. D., and Grottoli, A. (2010). Photo accolimatization by the coral *Montastraea cavernosa* in the mesophotic zone: light, food, and genetics. *Ecology* 91, 990–1003. doi: 10.1890/09-0313.1

Lewis, J. B., and Price, W. S. (1975). Feeding mechanisms and feeding strategies of Atlantic reef corals. *J. Zoology* 176, 527–544. doi: 10.1111/j.1469-7998.1975.tb03219.x

López-Londoño, T., Gómez-Campo, K., Hernández-Pech, X., Enríquez, S., and Iglesias-Prieto, R. (2022). Photosynthetic usable energy explains vertical patterns of biodiversity in zooxanthellate corals. *Sci. Rep.* 12, 20821. doi: 10.1038/s41598-022-25094-5

Loya, Y., Eyal, G., Treibitz, T., Lesser, M. P., and Appeldoorn, R. (2016). Theme section on mesophotic coral ecosystems: advances in knowledge and future perspectives. *Coral Reefs* 35, 1–9. doi: 10.1007/s00338-016-1410-7

Loya, Y., Puglise, K. A., and Bridge, T. C. K. (2019). *Mesophotic coral ecosystems* (Switzerland: Springer Nature).

Marsh, J. A. (1970). Primary productivity of reef-building calcareous red algae. *Ecology* 51, 255–263. doi: 10.2307/1933661

Martinez, S., Kolodny, Y., Shemesh, E., Scucchia, F., Nevo, R., Levin-Zaidman, S., et al. (2020). Energy sources of the depth-generalist mixotrophic coral *Stylophora pistillata*. *Front. Mar. Sci.* 7. doi: 10.3389/fmars.2020.566663

Mass, T., Kline, D. I., Roopin, M., Veal, C. J., Cohen, S., Iluz, D., et al. (2010). The spectral quality of light is a key driver of photosynthesis and photoadaptation in *Stylophora pistillata* colonies from different depths in the red Sea. *J. Exp. Biol.* 213, 4084–4091. doi: 10.1242/jeb.039891

McCree, K. J. (1981). "Photosynthetically active radiation," in *Physiological plant ecology I: responses to the physical environment*. Eds. O. L. Lange, P. S. Nobel, C. B. Osmond and H. Ziegler (Berlin, Heidelberg: Springer Berlin Heidelberg).

Minagawa, M., and Wada, E. (1984). Stepwise enrichment of $\delta^{15}N$ along food chains: further evidence and the relation between $\delta^{15}N$ and animal age. *Geochimica Cosmochimica Acta* 48, 1135–1140. doi: 10.1016/0016-7037(84)90204-7

Miyake, Y., and Wada, E. (1967). The abundance ratio of $^{15}N/^{14}N$ in marine environments. *Records Oceanogrphic Works Japan* 9.

Morrow, K. M., Fiore, C. L., and Lesser, M. P. (2016). Environmental drivers of microbial community shifts in the giant barrel sponge, *Xestospongia muta*, over a shallow to mesophotic depth gradient. *Environ. Microbiol.* 18, 2025–2038. doi: 10.1111/1462-2920.13226

Muir, P. R., and Pichon, M. (2019). "Biodiversity of reef-building scleractinian corals," in *Mesophotic coral ecosystems*. Eds. Y. Loya, K. A. Puglise and T. Bridge (Switzerland: Springer Nature).

Muir, P., Wallace, C., Bridge, T. C. L., and Bongaerts, P. (2015). Diverse staghorn coral fauna on the mesophotic reefs of north-east Australia. *PLoS One* 10, e0117933–e0117933. doi: 10.1371/journal.pone.0117933

Muller-Parker, G., D'Elia, C. F., and Cook, C. B. (2015). *Interactions between corals and their symbiotic algae* (Dordrecht: Springer).

Mullin, M. M., Rau, G. H., and Eppley, R. W. (1984). Stable nitrogen isotopes in zooplankton: some geographic and temporal variations in the north pacific. *Limnology Oceanogr.* 29, 1267–1273. doi: 10.4319/lo.1984.29.6.1267

Muscatine, L., and D'Elia, C. F. (1978). The uptake, retention, and release of ammonium by reef corals. *Limnology oceanogr.* 23, 725–734. doi: 10.4319/lo.1978.23.4.0725

Muscatine, L., Porter, J. W., and Kaplan, I. R. (1989). Resource partitioning by reef corals as determined from stable isotope composition. *Mar. Biol.* 100, 185–193. doi: 10.1007/BF00391957

Padilla-Gamiño, J. L., Roth, M. S., Rodrigues, L. J., Bradley, C. J., Bidigare, R. R., Gates, R. D., et al. (2019). Ecophysiology of mesophotic reef-building corals in hawai'i is influenced by symbiont–host associations, photoacclimatization, trophic plasticity, and adaptation. *Limnology Oceanogr.* 64, 1980–1995. doi: 10.1002/lno.11164

Palardy, J. E., Rodrigues, L. J., and Grottolic, A. G. (2008). The importance of zooplankton to the daily metabolic carbon requirements of healthy and bleached corals at two depths. *J. Exp. Mar. Biol. Ecol.* 376, 180–188. doi: 10.1016/j.jembe.2008.09.015

Pernice, M., Meibom, A., Heuvel, A. V. D., Kopp, C., Domart-Coulon, I., Hoegh-Guldberg, O., et al. (2012). A single-cell view of ammonium assimilation in coral–dinoflagellate symbiosis. *ISME J.* 6, 1314–1324. doi: 10.1038/ismej.2011.196

Peterson, B. J., and Fry, B. (1987). Stable isotopes in ecosystem studies. *Annu. Rev. Ecology Evolution Systematics* 18, 293–320. doi: 10.1146/annurev.es.18.110187.001453

Pichon, M. (2019). French Polynesia. In Mesophotic coral ecosystems. *Coral reefs of the world*. (Springer), 12, 425–443. doi: 10.1007/978-3-319-92735

Pinheiro, H. T., Eyal, G., Shepherd, B., and Rocha, L. A. (2019). Ecological insights from environmental disturbances in mesophotic coral ecosystems. *Ecosphere* 10, e02666–e02n/a. doi: 10.1002/ecs2.2666

Pochon, X., Forsman, Z. H., Spalding, H. L., Padilla-Gamiño, J. L., Smith, C. M., and Gates, R. D. (2015). Depth specialization in mesophotic corals (*Leptoseris* spp.) and associated algal symbionts in hawai'i. *R. Soc. Open Sci.* 2 (2), 140351. doi: 10.1098/rsos.140351

Price, J. T., McLachlan, R. H., Jury, C. P., Toonen, R. J., and Grottoli, A. G. (2021). Isotopic approaches to estimating the contribution of heterotrophic sources to Hawaiian corals. *Limnol. Oceanogr.* 66 (6), 2393–2407.

Qi, H., Coplen, T. B., Geilmann, H., Brand, W. A., and Böhlke, J. K. (2003). Two new organic reference materials for $\delta^{13}C$ and $\delta^{15}N$ measurements and a new value for the $\delta^{13}C$ of NBS 22 oil. *Rapid Commun. Mass Spectrometry* 17, 2483–2487. doi: 10.1002/rcm.1219

Radecker, N., Pogoreutz, C., Voolstra, C. R., Wiedenmann, J., and Wild, C. (2015). Nitrogen cycling in corals: the key to understanding holobiont functioning? *Trends Microbiol.* 23, 490–497. doi: 10.1016/j.tim.2015.03.008

Radice, V. Z., Brett, M. T., Fry, B., Fox, M. D., Hoegh-Guldberg, O., and DOVE, S. G. (2019a). Evaluating coral trophic strategies using fatty acid composition and indices. *PLoS One* 14, e0222327. doi: 10.1371/journal.pone.0222327

Radice, V. Z., Fry, B., Brown, K. T., Dove, S., and Hoegh-Guldberg, O. (2022). Biogeochemical niches and trophic plasticity of shallow and mesophotic corals recovering from mass bleaching. *Limnology Oceanogr.* 67, 1617–1630. doi: 10.1002/lno.12157

Radice, V. Z., Fry, B., Dove, S. G., and Hoegh-Guldberg, O. (2021). Biogeochemical variability and trophic status of reef water column following a coral bleaching event. *Coral reefs* 40, 1–7. doi: 10.1007/s00338-020-02021-6

Radice, V. Z., Hoegh-Guldberg, O., Fry, B., Fox, M. D., and Dove, S. G. (2019b). Upwelling as the major source of nitrogen for shallow and deep reef-building corals across an oceanic atoll system. *Funct. Ecol.* 33, 1120–1134. doi: 10.1111/1365-2435.13314

Ralph, P. J., Hill, R., Doblin, M. A., and Davy, S. K. (2015). "Theory and application of pulse amplitude modulated chlorophyll fluorometry in coral health assessment," in *Diseases of coral*. Eds. M. Cheryl, C. M. Woodley, C. A. Downs, A. W. Bruckner, J. W. Porter and S. B. Galloway (Hoboken, New Jersey, United States: John Wiley & Sons), 506–523.

Ralph, P. J., Schreiber, U., Gademann, R., Kuhl, M., and Larkum, A. W. D. (2005). Coral photobiology studied with a new imaging pulse amplitude modulated fluorometer. *J. Phycology* 41, 335–342. doi: 10.1111/j.1529-8817.2005.04034.x

Rangel, M. S., Erler, D., Tagliafico, A., Cowden, K., Scheffers, S., and Christidis, L. (2019). Quantifying the transfer of prey $\delta^{15}N$ signatures into coral holobiont nitrogen pools. *Mar. Ecol. Prog. Ser.* 610, 33–49. doi: 10.3354/meps12847

Reynaud, S., Ferrier-Pagès, C., Sambrotto, J.-L., Jaubert, J., and Gattuso, J.-P. (2002). Effect of feeding on the carbon and oxygen isotopic composition in the tissues and skeleton of the zooxanthellate coral *Stylophora pistillata*. *Mar. Ecol. Prog. Ser.* 238, 81–89. doi: 10.3354/meps238081

Reynaud, S., Martinez, P., and Houlbrèque, F. (2009). Effect of light and feeding on the nitrogen isotopic composition of a zooxanthellate coral: role of nitrogen recycling. *Mar. Ecol. Prog. Ser.* 392, 103–110. doi: 10.3354/meps08195

Richards, Z. T., Sampey, A., and Marsh, L. (2014). Kimberley Marine biota. historical data: scleractinian corals. *Records Western Aust. Museum Supplement* 84, 111–132. doi: 10.18195/issn.0313-122x.84.2014.111-132

Riegl, B., and Piller, W. E. (2003). Possible refugia for reefs in times of environmental stress. *Int. J. Earth Sci.* 92, 520–531. doi: 10.1007/s00531-003-0328-9

Rodrigues, L. J., and Grottoli, A. G. (2006). Calcification rate and the stable carbon, oxygen, and nitrogen isotopes in the skeleton, host tissue, and zooxanthellae of bleached and recovering Hawaiian corals. *Geochimica Cosmochimica Acta* 70, 2781–2789. doi: 10.1016/j.gca.2006.02.014

Rouzé, H., Galand, P. E., Medina, M., Bongaerts, P., Pichon, M., Pérez-Rosales, G., et al. (2021). Symbiotic associations of the deepest recorded photosynthetic scleractinian coral (172 m depth). *ISME J.* 15 (5), 1564–1568. doi: 10.1038/s41396-020-00857-y

RStudio Team (2020). *Integrated development for R* (Boston, MA: R Studio: PBC). Available at: http://www.RSTUDIO.com/.

Schlichter, D., Fricke, H. W., and Weber, W. (1986). Light harvesting by wavelength transformation in a symbiotic coral of the Red Sea twilight zone. *Mar. Biol.* 91, 403–407. doi: 10.1007/BF00428634

Schreiber, U. (2004). "Pulse-Amplitude-Modulation (PAM) fluorometry and saturation pulse method: an overview," in *Chlorophyll a fluorescence: a signature of photosynthesis*. Eds. G. C. Papageorgiou and Govindjee, (Netherlands: Springer).

Sebens, K. P., Vandersall, K. S., Savina, L. A., and Graham, K. R. (1996). Zooplankton capture by two scleractinian corals, *Madracis mirabilis* and *Montastrea cavernosa*, in a field enclosure. *Mar. Biol.* 127, 303–317. doi: 10.1007/BF00942116

Seemann, J. (2013). The use of ^{13}C and ^{15}N isotope labeling techniques to assess heterotrophy of corals. *J. Exp. Mar. Biol. Ecol.* 442, 88–95. doi: 10.1016/j.jembe.2013.01.004

Seemann, J., Carballo-Bolaños, R., Berry, K. L., González, C. T., Richter, C., and Leinfelder, R. R. (2012). "Importance of heterotrophic adaptations of corals to maintain energy reserves," in *Proceedings of the 12th International Coral Reef Symposium*, Cairns, Australia, 19A, pp. 9–13. Available at: http://www.icrs2012.com/proceedings/manuscripts/ICRS2012_19A_4.pdf.

Serrano, X., Baums, I. B., O'reilley, K., Smith, T. B., Jones, R. J., Shearer, T. L., et al. (2014). Geographic differences in vertical connectivity in the Caribbean coral *Montastraea cavernosa* despite high levels of horizontal connectivity at shallow depths. *Mol. Ecol.* 23, 4226–4240. doi: 10.1111/mec.12861

Sigman, D. M., Difiore, P. J., Hain, M. P., Deutsch, C., Wang, Y., Karl, D. M., et al. (2009). The dual isotopes of deep nitrate as a constraint on the cycle and budget of

oceanic fixed nitrogen. *Deep-sea Res. Part I Oceanographic Res. papers* 56, 1419–1439. doi: 10.1016/j.dsr.2009.04.007

Sigman, D. M., and Fripiat, F. (2019). Nitrogen isotopes in the ocean. *Encyclopedia Ocean Sci* (Elsevier) 263–278. doi: 10.1016/B978-0-12-409548-9.11605-7

Sturaro, N., Hsieh, Y. E., Chen, Q., Wang, P.-L., and Denis, V. (2019). Toward a standardised protocol for the stable isotope analysis of scleractinian corals. *Rapid Commun. Mass Spectrometry* 34, e8663. doi: 10.1002/rcm.8663

Sturaro, N., Hsieh, Y. E., Chen, Q., Wang, P.-L., and Denis, V. (2021). Trophic plasticity of mixotrophic corals under contrasting environments. *Funct. Ecol.* 35, 2841–2855. doi: 10.1111/1365-2435.13924

Sutton, D. C., and Hoegh-Guldberg, O. (1990). Host-zooxanthella interactions in four temperate marine invertebrate symbioses: assessment of effect of host extracts on symbionts. *Biol. Bull.* 178, 175–186. doi: 10.2307/1541975

Swart, P. K. (1983). Carbon and oxygen isotope fractionation in scleractinian corals: a review. *Earth-Science Rev.* 19, 51–80. doi: 10.1016/0012-8252(83)90076-4

Tamir, R., Eyal, G., Kramer, N., Laverick, J. H., and Loya, Y. (2019). Light environment drives the shallow-to-mesophotic coral community transition. *Ecosphere* 10 (9), e02839. doi: 10.1002/ecs2.2839

Tremblay, P., Maguer, J. F., Grover, R., and Ferrier-Pagès, C. (2015). Trophic dynamics of scleractinian corals: stable isotope evidence. *J. Exp. Biol.* 218, 1223–1234. doi: 10.1242/jeb.115303

Turner, J. A., Babcock, R. C., Hovey, R., and Kendrick, G. A. (2017). Deep thinking: a systematic review of mesophotic coral ecosystems. *ICES J. Mar. Sci.* 74, 2309–2320. doi: 10.1093/icesjms/fsx085

Turner, J. A., Babcock, R. C., Hovey, R., and Kendrick, G. A. (2018). AUV-based classification of benthic communities of the ningaloo shelf and mesophotic areas. *Coral Reefs* 37, 7630778. doi: 10.1007/s00338-018-1700-3

Veal, C. J., Holmes, G., Nunez, M., Hoegh-Guldberg, O., and Osborn, J. (2010). A comparative study of methods for surface area and threedimensional shape measurement of coral skeletons. *Limnology Oceanogr.: Methods* 8, 241–253. doi: 10.4319/lom.2010.8.241

Veron, J. E. N. (2000). *Corals of the world* (Australia: AIMS Publishing).

Vize, P. D. (2006). Deepwater broadcast spawning by *Montastraea cavernosa*, *Montastraea franksi*, and *Diploria strigosa* at the flower garden banks, gulf of Mexico. *Coral reefs* 25, 169–171. doi: 10.1007/s00338-005-0082-5

Whitaker, J. R., and Granum, P. E. (1980). An absolute method for protein determination based on difference in absorbance at 235 and 280 *nm*. *Analytical Biochem.* 109, 156–159. doi: 10.1016/0003-2697(80)90024-X

Zanden, M. J. V., and Rasmussen, J. B. (2001). Variation in δ^{15}N and δ^{13}C trophic fractionation: implications for aquatic food web studies. *Limnology Oceanogr.* 46, 2061–2066. doi: 10.4319/lo.2001.46.8.2061

Ziegler, M., Roder, C. M., Büchel, C., and Voolstra, C. R. (2015). Mesophotic coral depth acclimatization is a function of host-specific symbiont physiology. *Mar. Mol. Biol. Ecol.* 2. doi: 10.3389/fmars.2015.00004